# Elastically driven polaron patterns: Stripes and glass phases

P. Maniadis, T. Lookman, and A. R. Bishop
*Theoretical Division and Center for Nonlinear Studies, Los Alamos National Laboratory, Los Alamos, New Mexico 87545, USA*
(Received 8 March 2011; published 18 July 2011)

We investigate a model of elasticity-driven polaron pattern formation on a two-dimensional lattice at finite temperatures. We show that, at high densities, polaron stripes (glass-like) form when the gas is cooled. These stripes melt to a polaron gas upon heating. We attribute the emergent behavior to the role of the long-range, directional elastic interactions that favor a minimum in energy for polaron stripe formation.

DOI: 10.1103/PhysRevB.84.024304 PACS number(s): 63.20.Pw, 62.20.−x, 71.38.Ht, 05.10.Ln

## I. INTRODUCTION

Ceramic materials such as cuprates and manganites (and other transition-metal oxides) exhibit novel properties of high-temperature superconductivity, colossal magnetoresistance, ferromagnetism, and antiferromagnetism as well as multiferrocity.[1–11] In many of these materials, the competition between long- and short-range forces leads to the formation of long-range-ordered charge, spin, and lattice structures such as stripes and domain walls,[2,3] as well as self-organized and emergent properties often mediated via the lattice.[1] Stripes have been observed in ferromagnetic,[12,13] ferroelectric,[14] superconducting,[2,3,15,16] as well as hybrid superconducting-antiferromagnetic materials[17] and narrow-band semiconductors.[18,19] It has been suggested that long-range correlations and resulting stripes in the electronic charge or spin density influences the response of the material to external controlling affecting the superconducting state,[2,3] colossal magnetoresistance,[8,20] or colossal stressoresistance.[9]

We have previously proposed[21] an approach to describe the formation of polarons in which the electronic charge couples to the elastic fields to create an effective long-range and directional interaction between polarons. At low polaron density and zero temperature, the ground state of the system is a polaron stripe. When these stripes are brought in contact with a heat bath, the stripe survives up to temperatures comparable to the pairing energies of the polarons; for large temperatures, the kinetic energy of the polarons is greater than the binding energy and the system behaves as a polaron gas; at much higher temperatures the individual polarons melt. We can also expect an intermediate-temperature regime, where we have small stripe segments and free polarons constantly moving and reorganizing, with a liquid-like behavior. To describe the interaction with the thermal bath, we use here a hybrid adiabatic method, where we update the position of the polarons using standard Monte Carlo (MC) techniques.[22] The electron density and the elastic fields are calculated self-consistently (with the Newton method introduced in Ref. [21]) for every Monte Carlo step. For large densities, because the self-consistent calculation of the electronic densities is very slow, we treat the density of each polaron as a delta function ($\Delta$ model) and only recalculate the updated elastic fields at every Monte Carlo step.

This paper is organized as follows. In the next section we describe the Ginzburg-Landau free energy and compatibility conditions for the description of the elastic medium, and the Holstein coupling of the elastic fields with the polaron wave functions. Next we present the self-consistent Monte Carlo method and the numerical results we obtained for the dynamics of the multipolaron system at finite temperatures. We conclude with a discussion of the different behaviors we observe (stripe, liquid, and gas) for polarons at different temperatures, and the formation of polaron-stripe glass upon rapid cooling. We also discuss the short- and long-range correlations reflected in the distribution of polaron cluster sizes and their pair distribution function. Our approach should be viewed as complementary to phenomenological long-range Coulomb fields introduced into polaron-ordering discussions (see, e.g., Ref. [23]) in that we self-consistently deduce the form of long-range elastic fields from lattice compatibility conditions in the presence of polarons.

## II. STRAIN DESCRIPTION OF POLARONS IN AN ELASTIC MEDIUM

For the description of the elastic substrate in two dimensions (2D) on a square lattice, we use symmetry-adapted principal strains

$$e_1 = \frac{1}{\sqrt{2}}(\epsilon_{xx}+\epsilon_{yy}), \quad e_2 = \frac{1}{\sqrt{2}}(\epsilon_{xx}-\epsilon_{yy}), \quad e_3 = \epsilon_{xy} = \epsilon_{yx}, \tag{1}$$

where $e_1$ is the compressional (or dilatational) strain, $e_2$ is the deviatoric strain, and $e_3$ is the simple shear strain associated with a unit cell. Restricting ourselves to small strains, $\epsilon_{ij} = \frac{1}{2}(\frac{\partial u_i}{\partial x_j} + \frac{\partial u_j}{\partial x_i})$ are the Lagrangian strains. The three strains in 2D are not independent but are related by the integrability or St. Venant compatibility constraint, which in terms of the symmetry-adapted strains becomes

$$G = (\partial_x^2 + \partial_y^2)e_1 - (\partial_x^2 - \partial_y^2)e_2 - \sqrt{8}\partial_x\partial_y e_3 = 0$$

(this is true only if there are no dislocations or broken bonds in the lattice[24]).

The elastic energy density for a homogeneous medium is given by

$$F_{\rm el} = \frac{A_1}{2}{e_1}^2 + \frac{A_2}{2}{e_2}^2 + \frac{A_3}{2}{e_3}^2,$$

where $A_1$, $A_2$, and $A_3$ are the elastic moduli and the three strains are independent. (For details about the elastic fields and the Ginzburg-Landau energy see Refs. [25 and 26]).

The charged particles are coupled to the elastic deformations of the lattice. For the interactions with the elastic

 

fields, as well as the interaction between polarons, we use an extension of the semiclassical Holstein polaron model with an additional hard-core repulsion (the model as well as details of the numerical method for the calculation of the stripes are given in Ref. [21] and references therein). The interaction is modeled by the Hamiltonian interaction density

$$H_{\text{int}} = \chi \sum_i |\Psi_i|^2 e_1, \tag{2}$$

where $\Psi_i = \Psi_i(\mathbf{r})$ is the wave function of the particle $i$ and $e_1$ is the isotropic, dilatational strain mode, and the hard-core interaction between the polarons is described by the Hamiltonian

$$H_c = \sum_{i \neq j} U_0 |\Psi_i|^2 |\Psi_j|^2, \tag{3}$$

with the parameter $U_0$ determining the strength of a contact interaction. The Schrödinger equation describing the polarons in the presence of the elastic field can be written as

$$i \frac{d\Psi_i}{dt} = -V\nabla^2 \Psi_i + \chi e_1 \Psi_i + U_0 \sum_j |\Psi_j|^2 \Psi_i, \tag{4}$$

where we choose the Planck constant, $\hbar = 1$ to rescale time and set $k_B = 1$, so that energy and temperatures are measured in units of the overlap integral $V$. The elastic fields and the electron wave functions have been calculated self-consistently using the method in Ref. [21] for predefined positions of the electron, and the arrangement in a single stripe corresponds to the minimum of the energy for the system. Here we perform the same calculation, but we use a Monte Carlo updating method to change the positions of the centers of the polarons to account for the interaction with a thermal bath.

## III. NUMERICAL SIMULATIONS

In our previous work,[21] we showed that the wave function of the polaron is very localized, whereas the elastic fields extend anisotropically to much longer range. Due to this sharp localization of the wave function, in addition to the self-consistent calculation of the polarons, we introduce a simplified calculation ($\Delta$ model) in which we assume that the wave function of each polaron is a delta function, and we only calculate the elastic fields for each MC step. We have performed the MC simulation with the self-consistent calculation of the polarons as well as the $\Delta$ model and find the same qualitative behavior—the difference we obtain in the average energy (for the same temperature and after a long MC simulation) is less than 5%. The advantage of the $\Delta$ model is that we avoid the computationally expensive self-consistent calculation of the polarons. The calculations presented in this paper are performed using the $\Delta$ model on a $55 \times 55$ lattice, but they are qualitatively the same as our calculations on smaller lattices and for small numbers of polarons using the full self-consistent calculation. For the Monte Carlo simulations we typically start at zero temperature with the polarons arranged in stripes, and we increase the temperature in small steps. For every temperature increment we perform 30 to 100 thousand Monte Carlo steps. We smooth the fluctuations of the energy curves by taking the average of the energy over 50 realizations. The energy as a function of temperature for different numbers of polarons is plotted in Fig. 1.

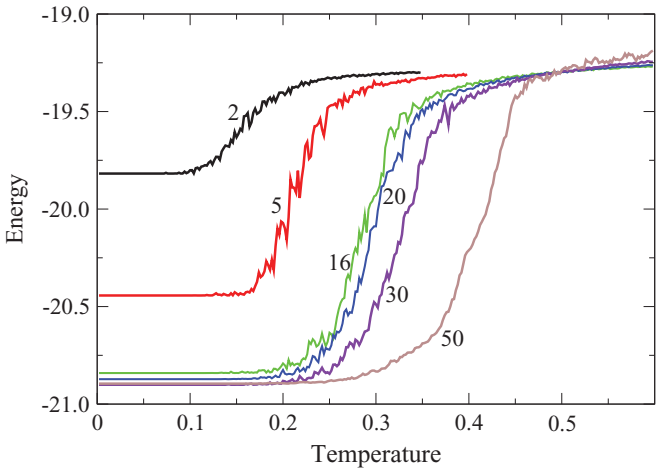


FIG. 1. (Color online) Monte Carlo results of the elastic energy with $N_p$ polarons on a $55 \times 55$ lattice as a function of temperature for $N_p = 2,5,16,30,50$.

As we see in Fig. 1, there is a transition interval in the energy as we increase the temperature from zero to 0.6. For two polarons, the low-temperature limit corresponds to a stable bound state, while the high-temperature limit corresponds to uncorrelated polaron motion. In the transition interval we observe the formation of unstable bound states, with a lifetime that decreases as the temperature increases.

Similar behavior is observed in systems with larger numbers of polarons, as we see in Figs. 1 and 2. At low temperature

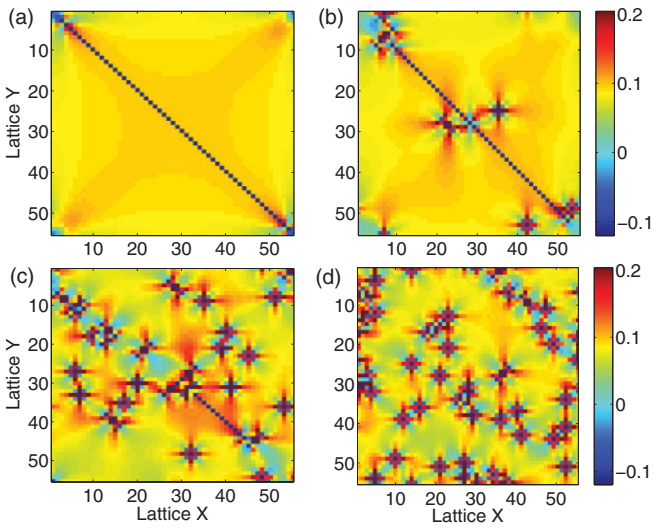


FIG. 2. (Color online) The strain $e_1$ for 50 polarons on a $55 \times 55$ lattice and for different temperatures. (a) Polaron stripe at zero temperature. (b) Low-temperature transition regime $T = 0.38$. The long stripe becomes unstable and a small number of polarons escape, moving alone or forming smaller stripes. (c) Intermediate-temperature transition regime with $T = 0.42$. The long stripe is almost completely destroyed. Individual polarons move on the lattice and form smaller stripes with a finite lifetime. (d) High-temperature regime with $T = 0.6$. All polarons move independently: Small stripes are formed but their lifetime is very short.

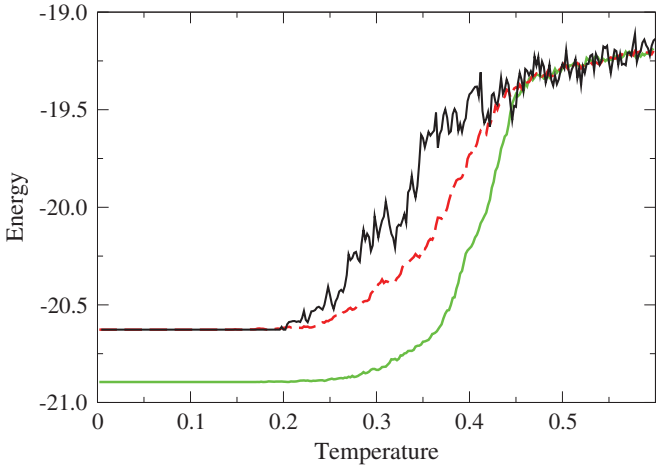


FIG. 3. (Color online) Hysteresis loop when a system of 55 polarons is cooled, starting with a thermalized polaron gas at high temperatures. The upper line is the energy when cooled from the polaron gas, while the lower line corresponds to the average energy upon heating the system starting with a stripe at $T = 0$. When the system is cooled, it freezes into a higher-energy glassy state with many smaller stripes. The dashed line is the average energy obtained by reheating the system starting from the frozen, many stripes glassy state obtained upon cooling.

we have a stable stripe. There is a transition at intermediate temperatures, and at high temperatures we have almost-independent polaron motion. We identify three regimes: (A) Below the transition temperature, we have stable stripes. (B) In the transition regime the stripe becomes unstable and breaks into smaller stripes and freely moving polarons, which continuously recombine to form other finite-lifetime stripe segments; in this temperature range, the polarons exhibit liquid-like behavior. (C) At high temperatures we have almost uncorrelated, gaslike polaron dynamics. In Fig. 2 we plot the $e_1$ strain for a system of 50 polarons on a 55 × 55 lattice.

As we can see in Fig. 2(b), at the beginning of the transition, a small number of polarons thermally escape from the large stripe. The number of polarons that escape increases as the temperature increases. These freed polarons can either move independently or they form smaller stripes with finite lifetime. This formation of small transient stripes, as well as the free polarons, can be seen in Figs. 2(b) and 2(c). The behavior of the polarons resembles that of liquids, where there is a short-range order with a finite lifetime. For high

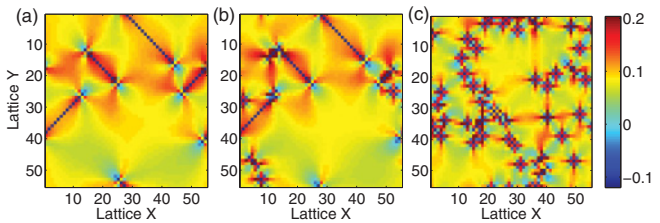


FIG. 4. (Color online) The strain field $e_1$ obtained from cooling an initially thermalized polaron gas at high $T$. (a) The frozen glassy state with many stripes ($T = 0$). (b) Intermediate temperature $T = 0.34$ where the glassy state is almost formed. (c) The initial high-temperature polaron gas for $T = 0.6$.

temperatures, the formation of transient stripes becomes rare, and their lifetime shrinks to few MC steps, as for a gas.

In Fig. 3 we plot the energy of the system with 50 polarons on a 55 × 55 lattice, when we slowly decrease the temperature (the temperature step is 0.001–0.005, and we perform 50–100 thousand Monte Carlo steps for every $T$) starting from the high-temperature polaron gas [Fig. 4(c)]. For comparison, we also plot the average energy when we heat, starting from the stripe ground state. When we decrease the temperature, depending on the cooling rate and the number of polarons, the system cannot easily reach the ground state to form a single stripe. This can only happen when the number of polarons is small (of the order of 10–15) and the cooling rate is slow (100 thousand Monte Carlo steps for each temperature step, with very small temperature steps). The energy landscape exhibits many local minima, each corresponding to a different stripe configuration, separated by energy barriers. The height of these barriers increases with the number of polarons. For a small number of polarons, the temperature fluctuations can overcome the barriers and the system relaxes faster to the absolute ground state. For a large number of polarons, or fast cooling rates, there is a hysteretic formation of many small stripes [Fig. 4(b)]. As the temperature decreases, the lifetime of these stripes increases and, as a result, the polarons are trapped into this metastable state [Fig. 4(a)]. As we see in Fig. 3, the energy of this metastable state is higher than the ground state, but the energy barrier separating it from the ground state is very large, limiting transitions between them.

From Figs. 2 and 4 we see that there is a formation of polaron clusters and the distribution of cluster sizes changes with temperature (see also movies in supplemental materials[27]). The distribution of cluster sizes is a robust delta function at low and high temperatures (centered around $N_p$ and 1, respectively). For intermediate temperatures the system exhibits a broad distribution of cluster sizes and associated

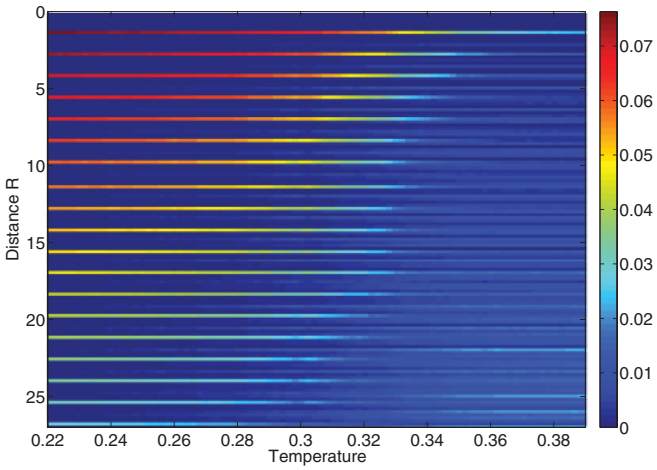


FIG. 5. (Color online) Pair distribution function density plot as a function of temperature for $N_p = 30$ on a 55 × 55 lattice. A regular arrangement of delta-function peaks with zero background fluctuations is seen for small temperatures, but as the temperature increases the long-range correlation becomes weaker and the corresponding peaks are replaced by a background fluctuation. At even higher temperatures, even the short-range correlations disappear and the pair distribution becomes almost uniform.

time scales. Multi-time scale responses are likely but beyond the statistics of our small system sizes.

We also calculate the pairdistribution function for the polarons and follow its changes with temperature. We start heating the system with the polarons arranged in the ground state of a single stripe for $T = 0$. At this temperature the pair distribution function consists of well-defined delta-function peaks. These peaks are seen in Fig. 5 as lines in the density plots. As the temperature increases, the long-range correlations disappear, and the peaks corresponding to large separation between the polarons decrease, while the background of the pair distribution function becomes more uniform. At higher temperatures, all the peaks disappear, and the pair distribution function becomes uniform (to the degree permitted by the discretization of our simulation box). As we see from Fig. 5, the correlation length of the stripe decreases, as we increase the temperature, from the total length of the stripe at $T = 0$ to zero at high temperatures. In the transition region the pair distribution function confirms that we have liquid-like behavior; there is no long-range correlation, but we do have short-range correlation, and the formation of smaller stripes. This is typical behavior of the pair distribution function for liquids.

## IV. CONCLUSION

We have used a classical Monte Carlo method to study the variations with temperature of a many-polaron system coupled adiabatically through an elastic substrate. The ground state of the system corresponds to the formation of an extended stripe, with all the polarons arranged parallel to the $\langle 11 \rangle$ direction of the underlying square lattice. When the temperature is increased, the system undergoes a transition from a single stable stripe to smaller metastable stripes with liquid-like behavior and, finally, at higher temperatures, to a weakly correlated polaron gas. When cooling this polaron gas, we observe the formation of a hysteretic glassy metastable state with many stripe segments at low temperature. There is a high energy barrier that does not allow the polarons to evolve from this glassy state to the single-stripe ground state. The formation of the glassy state depends on the cooling rate and the density of polarons. We also calculate the pair distribution function for the polarons, and find that, at intermediate temperatures, there is a short-range correlation but the long-range correlation is lost, consistent with a liquid-like phase. At higher temperatures, even the short-range correlation is lost, and the system behaves like a polaron gas.

## ACKNOWLEDGMENTS

This research was carried out under the auspices of the National Nuclear Security Administration of the US Department of Energy at Los Alamos National Laboratory under Contract No. DE-AC52-06NA25396.

[1] K. Ahn, T. Lookman, and A. Bishop, Nature (London) **428**, 401 (2004).
[2] S. W. Cheong, G. Aeppli, T. E. Mason, H. Mook, S. M. Hayden, P. C. Canfield, Z. Fisk, K. N. Clausen, and J. L. Martinez, Phys. Rev. Lett. **67**, 1791 (1991).
[3] J. Tranquada, B. Sternlieb, J. Axe, Y. Nakamura, and S. Uchida, Nature (London) **375**, 561 (1995).
[4] E. Dagoto, *Nanoscale Phase Separation and Colossal Magnetoresistance* (Springer-Verlag, 2003).
[5] A. R. Bishop, S. R. Shenoy, and S. E. Sridhar, *Intrinsic Multiscale Structure and Dynamics in Complex Electronic Oxides* (World Scientific, Singapore, 2003).
[6] A. Bishop, T. Lookman, A. Saxena, and S. Shenoy, Europhys. Lett. **63**, 289 (2003).
[7] T. Kimura, T. Goto, H. Shintani, K. Ishizaka, T. Arima, and Y. Tokura, Nature (London) **426**, 55 (2003).
[8] N. Mathur and P. Littlewood, Phys. Today **56**, 25 (2003).
[9] H. Y. Hwang, T. T. M. Palstra, S. W. Cheong, and B. Batlogg, Phys. Rev. B **52**, 15046 (1995).
[10] M. Fäth, S. Freisem, A. Menovsky, Y. Tomioka, J. Aarts, and J. Mydosh, Science **285**, 1540 (1999).
[11] V. Emery and S. Kivelson, Physica C **235**, 189 (1994).
[12] O. Portmann, A. Vaterlaus, and D. Pescia, Nature (London) **422**, 701 (2003).
[13] C. Helman, J. Milano, S. Tacchi, M. Madami, G. Carlotti, G. Gubbiotti, G. Alejandro, M. Marangolo, D. Demaille, V. H. Etgens *et al.*, Phys. Rev. B **82**, 094423 (2010).
[14] S. K. Streiffer, J. A. Eastman, D. D. Fong, C. Thompson, A. Munkholm, M. V. Ramana Murty, O. Auciello, G. R. Bai, and G. B. Stephenson, Phys. Rev. Lett. **89**, 67601 (2002).
[15] J. Park, D. Inosov, C. Niedermayer, G. Sun, D. Haug, N. Christensen, R. Dinnebier, A. Boris, A. Drew, L. Schulz *et al.*, Phys. Rev. Lett. **102**, 117006 (2009).
[16] L. P. Gor'kov and G. B. Teitel'baum, Phys. Rev. B **82**, 020510 (2010).
[17] K. Kitagawa, N. Katayama, H. Gotou, T. Yagi, K. Ohgushi, T. Matsumoto, Y. Uwatoko, and M. Takigawa, Phys. Rev. Lett. **103**, 257002 (2009).
[18] F. V. Kusmartsev, Phys. Rev. Lett. **84**, 530 (2000).
[19] F. Kusmartsev, Phys. Rev. Lett. **84**, 5026 (2000).
[20] *Colossal Magnetoresistance and Related Properties*, edited by B. Raveau and C. Rao (World Scientific, Singapore, 1998).
[21] P. Maniadis, T. Lookman, and A. R. Bishop, Phys. Rev. B **78**, 134304 (2008).
[22] R. Rubinstein and D. Kroese, *Simulation and the Monte Carlo Method* (Wiley Interscience, 2008).
[23] T. Mertelj, V. V. Kabanov, and D. Mihailovic, Phys. Rev. Lett. **94**, 147003 (2005).
[24] R. Gröger, T. Lookman, and A. Saxena, Phys. Rev. B **78**, 184101 (2008).
[25] T. Lookman, S. R. Shenoy, K. O. Rasmussen, A. Saxena, and A. R. Bishop, Phys. Rev. B **67**, 024114 (2003).
[26] S. R. Shenoy, T. Lookman, A. Saxena, and A. R. Bishop, Phys. Rev. B **60**, R12537 (1999).
[27] See Supplemental Material at http://link.aps.org/supplemental/10.1103/PhysRevB.84.024304 for movies generated from the Monte Carlo simulations for $N_p = 50$ and for different temperatures (2011).